

“New Cathode Materials for Intermediate Temperature Solid Oxide Fuel Cells”  
Quarterly Report for 1/1/2004 to 3/31/2004

DE-FC26-03NT41960

May 11, 2004

Allan J Jacobson  
Center for Materials Chemistry  
University of Houston  
Houston, Texas 77204-5003

*“This report was prepared as an account of work sponsored by an agency of the United States Government. Neither the United States Government nor any agency thereof, nor any of their employees, makes any warranty, express or implied, or assumes any legal liability or responsibility for the accuracy, completeness, or usefulness of any information, apparatus, product, or process disclosed, or represents that its use would not infringe privately owned rights. Reference herein to any specific commercial product, process, or service by trade name, trademark, manufacturer, or otherwise does not necessarily constitute or imply its endorsement, recommendation, or favoring by the United States Government or any agency thereof. The views and opinions of authors expressed herein do not necessarily state or reflect those of the United States Government or any agency thereof.”*

## Abstract

Operation of SOFCs at intermediate temperatures (500 – 800 °C) requires new combinations of electrolyte and electrode materials that will provide both rapid ion transport across the electrolyte and electrode - electrolyte interfaces and efficient electrocatalysis of the oxygen reduction and fuel oxidation reactions. This project concentrates on materials and issues associated with cathode performance that are known to become limiting factors as the operating temperature is reduced.

The specific objectives of the proposed research are to develop cathode materials that meet the electrode performance targets of 1.0 W/cm<sup>2</sup> at 0.7 V in combination with YSZ at 700 °C and with GDC, LSGM or bismuth oxide based electrolytes at 600 °C. The performance targets imply an area specific resistance of ~0.5 Ωcm<sup>2</sup> for the total cell. The research strategy is to investigate both established classes of materials and new candidates as cathodes, to determine fundamental performance parameters such as bulk diffusion, surface reactivity and interfacial transfer, and to couple these parameters to performance in single cell tests.

The initial choices for study are perovskite oxides based on Sr substituted LaFeO<sub>3</sub>, where significant data in single cell tests exists at PNNL for cathodes on both YSZ and CSO/YSZ, and of Ln<sub>2</sub>NiO<sub>4</sub> compositions. A key component of the research strategy is to evaluate for each cathode material composition, the key performance parameters, including ionic and electronic conductivity, surface exchange rates, stability with respect to the specific electrolyte choice, and thermal expansion coefficients. Results on electrical conductivity relaxation measurements on La<sub>2</sub>NiO<sub>4+x</sub> and Pr<sub>2</sub>NiO<sub>4+x</sub> samples are reported and compared with results from previous studies. Studies of the crystallization of amorphous SrFeO<sub>3-x</sub> and LaFeO<sub>3-x</sub> films prepared by pulsed laser deposition are reported. Such studies are a preliminary to the combinatorial synthesis approach described in the first report.

## Table of Contents

1.	List of Graphical Materials	3
2.	Introduction	4
3.	Executive Summary	4
4.	Experimental	4
4.1	Characterization of K1 Compositions $\text{La}_2\text{NiO}_{4+x}$ and $\text{Pr}_2\text{NiO}_{4+x}$	4
4.2	DC Conductivity Measurements	5
4.3	Electrical Conductivity Relaxation Measurements	6
5.	Combinatorial Approach to Measurement of Transport Parameters.	8
5.1	Deposition and Crystallization of Amorphous Films of $\text{LaFeO}_3$ and $\text{SrFeO}_{2.5}$ .	9
6	Conclusions	10
7	References	10
8	List of Acronyms and Abbreviations	11
9	Milestones	11

## 1. List of Graphical Materials

Figure 1. Thermogravimetric Analysis Data for  $\text{La}_2\text{NiO}_{4+x}$ .  
Figure 2. The total conductivity of  $\text{La}_2\text{NiO}_{4+x}$  (left) and  $\text{Pr}_2\text{NiO}_{4+x}$  (right).  
Figure 3. Typical conductivity relaxation data for  $\text{La}_2\text{NiO}_{4+x}$ .  
Figure 4. Values of  $D_{\text{chem}}$  (left) and  $D_O$  (right) determined by Electrical Conductivity Relaxation.  
Figure 5. Comparison of the present results with the IEDP data of reference x and y  
Figure 6. Schematic of the Approach to Make Multiple Compositions on One Substrate.  
Figure 7. Temperature dependence of the resistance of amorphous  $\text{SrFeO}_{2.5}$  and  $\text{LaFeO}_3$  films.

## 2. Introduction

The objectives of the project are to discover new oxide cathode materials that meet a performance target of  $1.0 \text{ W/cm}^2$  at  $0.7 \text{ V}$  in combination with YSZ at  $700 \text{ }^\circ\text{C}$  and with CGO, LSGM electrolytes at  $600 \text{ }^\circ\text{C}$ . An ancillary objective of the project is to increase fundamental understanding of the intrinsic transport properties of mixed electronic ionic conducting oxides and oxide-oxide interfaces that can be used to accelerate further progress in the development of cost effective high performance solid oxide fuel cells. In Phase I, we are measuring the surface exchange rates, diffusion coefficients and interfacial transport for an initial set of perovskite related oxide materials. In Phase II we will synthesize and characterize new cathode materials and measure their kinetic parameters. The thermal and chemical compatibility with different electrolytes will be determined. Based on the results, a subset of the best materials will be selected for single cell tests. The phase III objectives are to evaluate the performance of the best materials identified in Phase I and II. The optimum electrode composition and microstructure will be determined and the longer term performance characteristics evaluated.

## 3. Executive Summary

The project began on October 1, 2003 and this is the second quarterly report. In the second period, we have completed the stoichiometry measurements on the  $\text{Ln}_2\text{MO}_4$ <sup>1-9</sup> phases  $\text{La}_2\text{NiO}_{4+x}$  and  $\text{Pr}_2\text{NiO}_{4+x}$  in different oxygen partial pressures. We have measured the dc conductivities as a function of  $\text{pO}_2$  in several oxygen partial pressures. We have made preliminary electrical conductivity relaxation measurements as function of temperature for several different  $\text{pO}_2$  switches. From these data and the stoichiometry measurements, values of the diffusion and surface exchange coefficients have been extracted. The results are compared with data obtained by isotope exchange and depth profiling. We have also started to prepare thin oxide films by pulsed laser deposition for study of transport kinetics. We have decided to adopt a combinatorial approach, initially with the  $\text{LaFeO}_3 - \text{SrFeO}_{2.5}$  system to determine synthesis and evaluation conditions. Thin film samples of both compositions have been made in amorphous form and the crystallization behavior determined.

## 4. Experimental

### 4.1 Characterization of K1 Compositions $\text{La}_2\text{NiO}_{4+x}$ and $\text{Pr}_2\text{NiO}_{4+x}$

The syntheses and compositional characterization of  $\text{La}_2\text{NiO}_{4+x}$  and  $\text{Pr}_2\text{NiO}_{4+x}$  were described in the previous report.

A TA Instruments 2950 thermobalance was used to determine the equilibrium non-stoichiometry and thermodynamic factor ( $\Gamma$ ) as a function of temperature and oxygen partial pressure within the range of  $0.01 \leq \text{pO}_2 \leq 0.07 \text{ atm}$  and  $25 \text{ }^\circ\text{C} \leq T \leq 950 \text{ }^\circ\text{C}$ . Similar results have been completed for  $\text{La}_2\text{NiO}_{4+x}$  and  $\text{Pr}_2\text{NiO}_{4+x}$ . The results are shown in Figure 1 for the two compositions. In the temperature range of interest,  $500-700 \text{ }^\circ\text{C}$ , both compositions have significant concentrations of interstitial oxygen ions. At the same

temperature and  $pO_2$  the interstitial oxygen ion concentration is greater in  $Pr_2NiO_{4+x}$  than in  $La_2NiO_{4+x}$ .

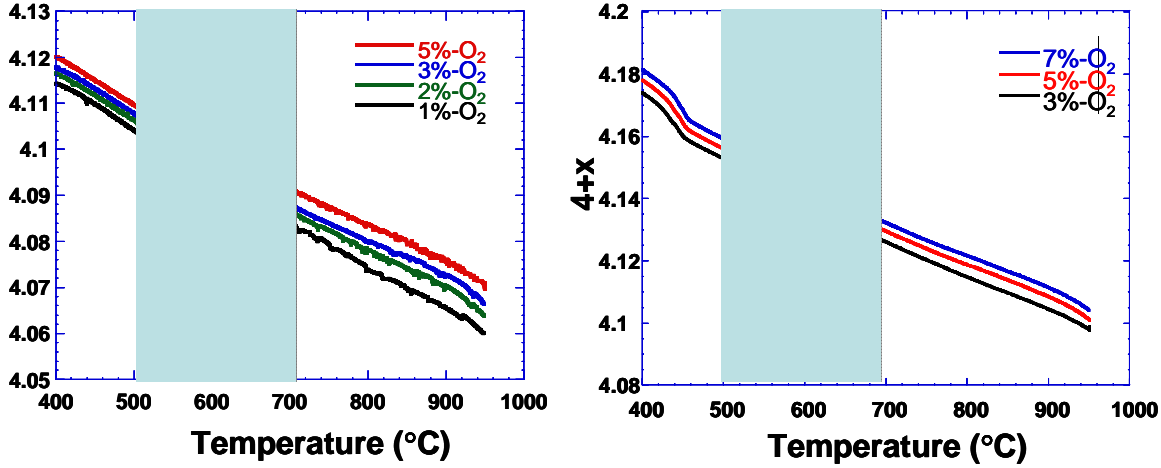


Figure 1. Thermogravimetric Analysis Data for  $La_2NiO_{4+x}$ .

#### 4.2 DC Conductivity Measurements

Rectangular shaped bars for  $La_2NiO_{4+x}$  ( $16.0 \times 1.6 \times 1.7$  mm) and for  $Pr_2NiO_{4+x}$  ( $18.0 \times 1.8 \times 2.1$  mm) were cut for DC conductivity and electrical conductivity relaxation (ECR) measurements. The length is made much longer than the width and the thickness for ECR measurements. The densities of the bars measured by the Archimedes method were 95 % for  $La_2NiO_{4+x}$  and 96 % for  $Pr_2NiO_{4+x}$  relative to the theoretical densities.

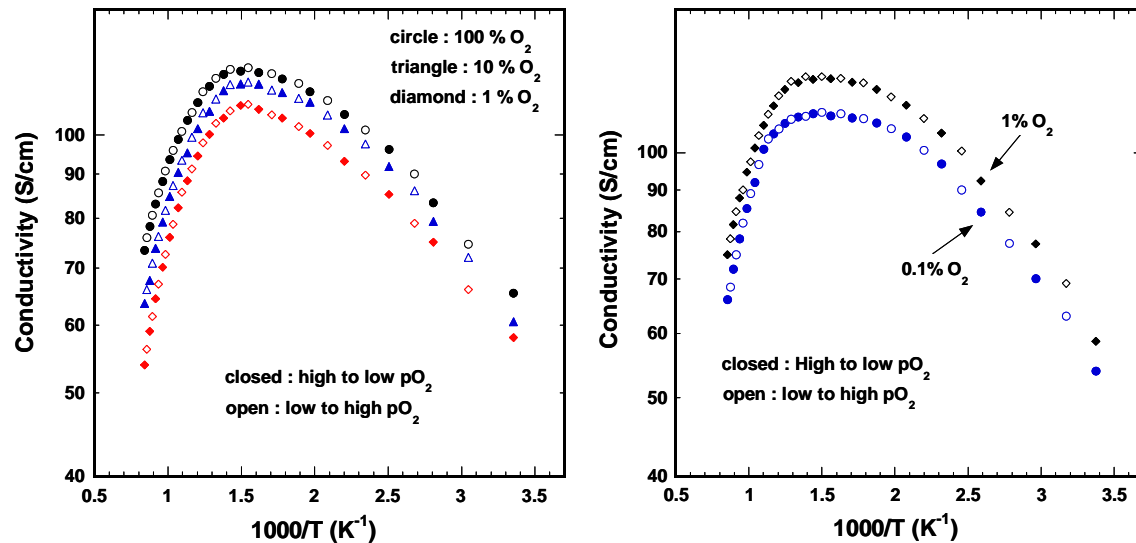


Figure 2. The total conductivity of  $La_2NiO_{4+x}$  (left) and  $Pr_2NiO_{4+x}$  (right).

The total conductivity results are shown in Figure 2. The data show typical behavior for p-type conductors that lose oxygen atoms on heating. At near ambient temperature, the

data show Arrhenius behavior but above  $\sim 200$   $^{\circ}\text{C}$ , the rate of increase of the conductivity begins to decrease. This temperature is about 100-150  $^{\circ}\text{C}$  lower than most perovskite oxides implying faster oxygen exchange kinetics. The maximum conductivity in both cases is about  $200 \text{ Scm}^{-1}$ , a reasonable value for use of the materials as SOFC cathodes.

#### 4.3 Electrical Conductivity Relaxation Measurements

Electrical conductivity relaxation measurements were made using an experimental apparatus and analysis procedure that we have previously reported.<sup>10</sup> A typical relaxation curve for  $\text{La}_2\text{NiO}_{4+x}$  is shown in Figure 3 for a pressure switch between 0.01 and 0.02 atm at 800  $^{\circ}\text{C}$ . The open symbols are the data and the continuous line the experimental fit with two parameters  $D_{\text{chem}}$  and  $k_{\text{chem}}$ . The difference between the data and the calculated fit are shown also (error) and indicate excellent agreement of the data with the model.

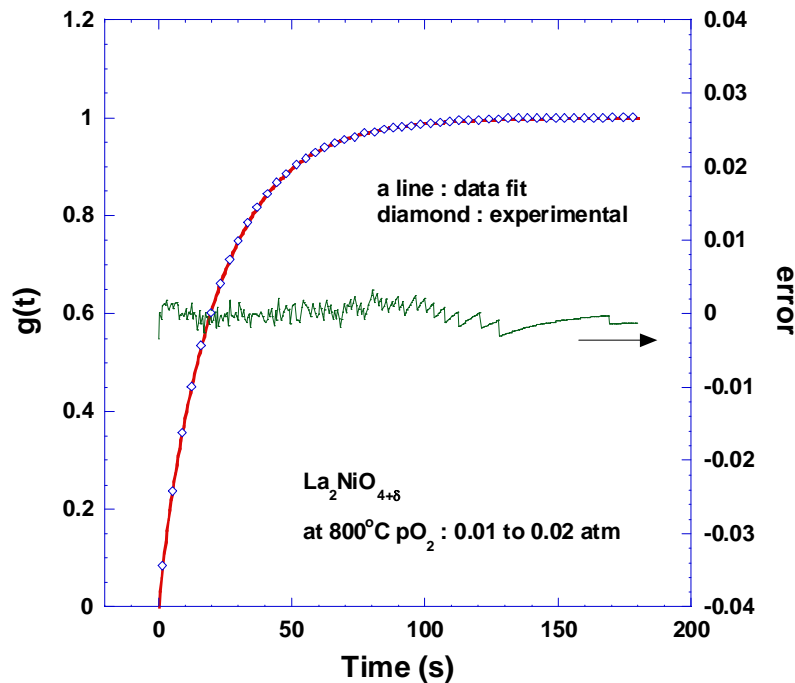


Figure 3. Typical conductivity relaxation data for  $\text{La}_2\text{NiO}_{4+x}$

Results for the chemical diffusion coefficient  $D_{\text{chem}}$  for several different pressure switches as a function of temperature are shown in Figure 4 (left) for both  $\text{La}_2\text{NiO}_{4+x}$  and  $\text{Pr}_2\text{NiO}_{4+x}$ . The results show some dependence on the final pressure of the switch in both cases. This is primarily associated with small changes in the thermodynamic factors in this pressure range. The pressure dependence disappears when the oxygen ion diffusion coefficients are calculated according to  $D_{\text{O}} = D_{\text{chem}} / \Gamma$  where  $\Gamma$  is the thermodynamic factor as shown in Figure 4 (right). It is apparent in Figure 4 that  $D_{\text{O}}$  for the praseodymium compound is higher than for  $\text{La}_2\text{NiO}_{4+x}$ . The values of  $D_{\text{O}}$  for both compounds have similar activation energies. In Figure 5, the present results are compared

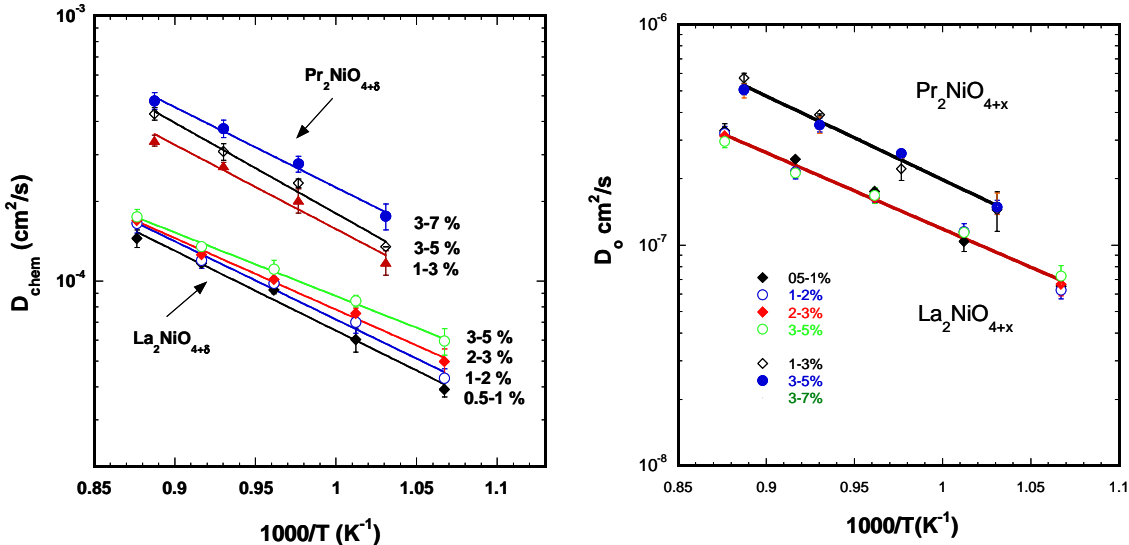


Figure 4. Values of  $D_{\text{chem}}$  (left) and  $D_o$  (right) determined by Electrical Conductivity Relaxation

with previous results obtained by isotope exchange and depth profiling (IEDP). The diffusion coefficients measured in the present work are comparable to the IEDP data which show the same trend in that  $D_o(\text{Pr}_2\text{NiO}_{4+x}) > D_o(\text{La}_2\text{NiO}_{4+x})$ . In contrast, the values of  $k_{\text{ex}}$  are quite different in both magnitude and activation energy. The reason for this is not yet known but is important because the  $k_{\text{ex}}$  values that we measure would be expected to give much lower electrode resistances. We will carry out additional AC impedance experiments to confirm our measured values. It is important to keep in mind that the surface exchange coefficient is likely to be sensitive to sample preparation conditions, surface compositions and the presence of impurity phases.

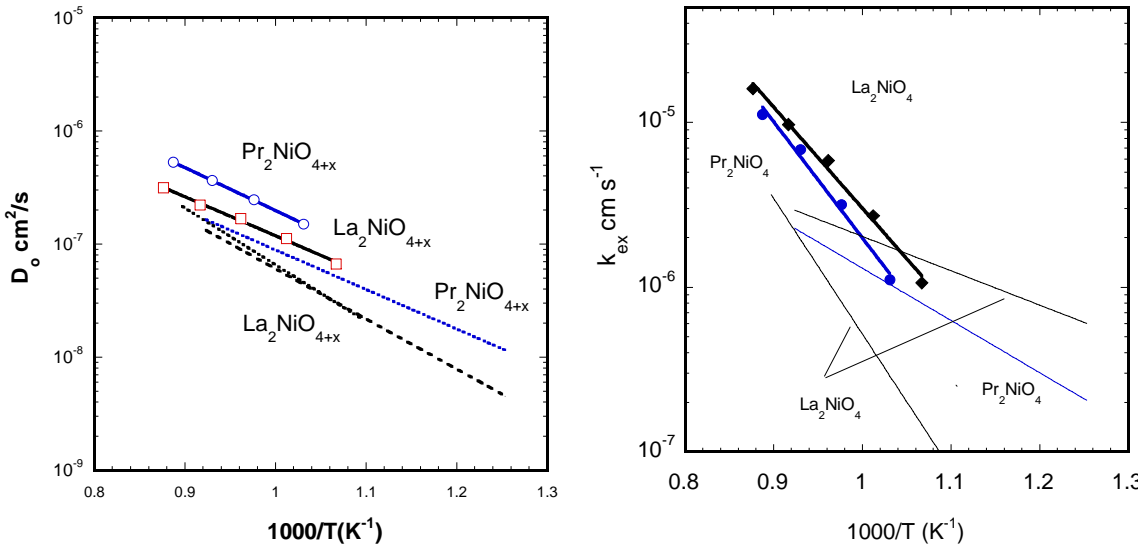


Figure 5. Comparison of the present results with the IEDP data of reference 3 and 11

## 5. Combinatorial Approach to Measurement of Transport Parameters.

Perovskite and perovskite - related oxides are noteworthy for their tolerance of a very wide range of compositions. This is an advantage in that variations in composition can be used to simultaneously optimize several important properties such as surface exchange rate, diffusion coefficient, thermal expansion, and substrate reactivity. The disadvantage is that the matrix of possible compositions is very large and serial evaluation of properties is time consuming. Consequently, we have decided to adopt a combinatorial approach whereby many compositions can be screened for one or more properties using a single specimen. As a first step, we plan to investigate compositions in the  $\text{LaFeO}_3$  –  $\text{SrFeO}_{2.5}$  system which have been shown recently to be of interest as cathode materials for intermediate temperature operation. Eventually, we plan to expand the scope to include four different oxide components. We will use the two oxide component system to develop the technique and the processing conditions needed to prepare samples and the evaluation techniques. Samples will be prepared in the form of thin films by pulsed laser deposition (PLD) on single crystal yttria stabilized zirconia substrates. The general approach is shown in Figure 5.

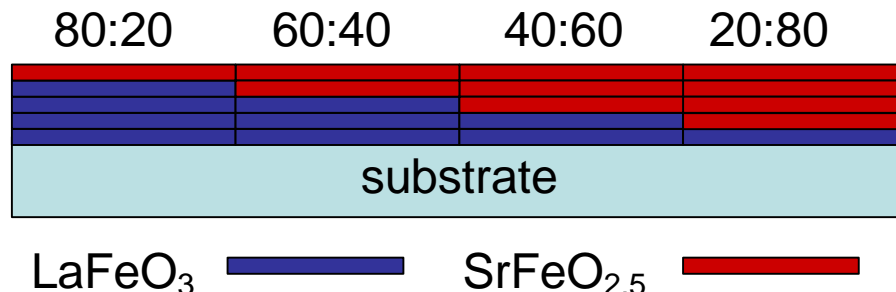


Figure 6. Schematic of the Approach to Make Multiple Compositions on One Substrate.

A shadow mask will be used to deposit the first oxide ( $\text{LaFeO}_3$  in Figure 5) in steps of different thickness. In a second step, the second oxide ( $\text{SrFeO}_{2.5}$  in Figure 5) will be deposited in reverse order to produce a film of uniform total thickness. The films will be deposited with the substrate at ambient temperature where they will be amorphous.

To date, we have synthesized the targets, constructed the mask, and begun to determine the deposition parameters. The initial film synthesis to determine the crystallization temperatures has been completed. (Task 5.1)

### 5.1 Deposition and Crystallization of Amorphous Films of $\text{LaFeO}_3$ and $\text{SrFeO}_{2.5}$ .

Amorphous films of  $\text{LaFeO}_3$  and  $\text{SrFeO}_{2.5}$  were deposited on (001)  $\text{MgO}$  substrates by pulsed laser ablation at room temperature in an atmosphere of 200 mTorr oxygen with stoichiometric targets. The resistances of the films were measured as a function of temperature in 1 atm  $\text{O}_2$  using the 4-probe technique. Four platinum leads of 0.001 in. diameter were mechanically mounted onto the film directly to serve as current and

voltage electrodes. No conductive glue was used to avoid experimental artifacts from possible reaction between conductive glue and the amorphous films. Current was provided by using a Keithley 2400 sourcemeter and was continuously adjusted during the measurement according to the resistance of the films. The voltage was measured using a Keithley 2000 multimeter. Films were slowly heated a rate of 1 °C/min. Six data points were collected for every degree increase so that fine features of the dynamics of crystallization and phase transitions were not missed.

In this quarter, we made thin amorphous films of  $\text{SrFeO}_{2.5}$  and  $\text{LaFeO}_3$  using pulsed laser deposition method. To determine the appropriate annealing procedure, we measured the resistance of films of both compounds as a function of temperature, since in general electrical transport properties reflects micro-structural characteristics of complex transition metal oxides. On the other hand, this method is faster and reveals more accurate information than using XRD alone because some transitions may occur at temperatures only a few degrees apart.

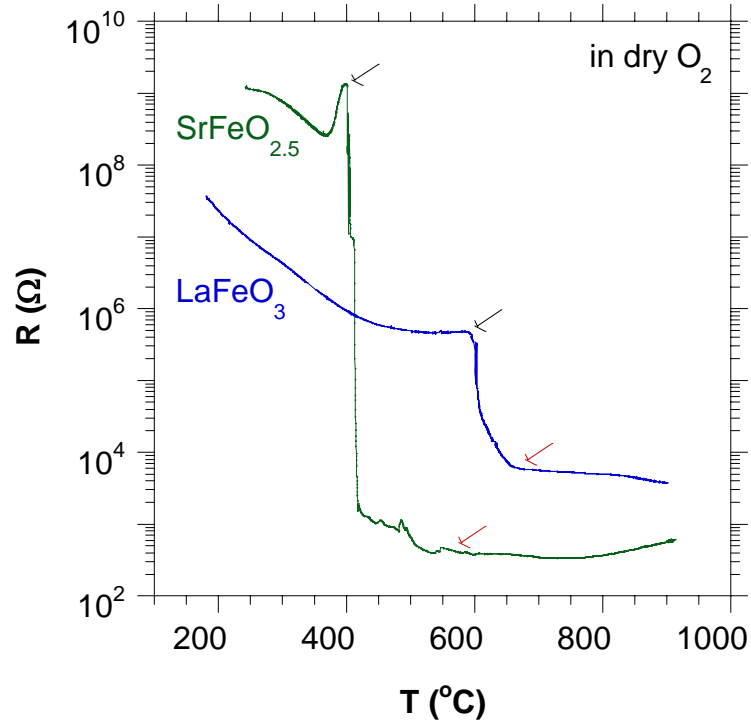


Figure 7. Temperature dependence of the resistance of amorphous  $\text{SrFeO}_{2.5}$  and  $\text{LaFeO}_3$  films.

The resistance of both amorphous  $\text{SrFeO}_{2.5}$  film and  $\text{LaFeO}_3$  film in dry oxygen is plotted as a function of temperature in Figure 1. The nucleation and crystallization process, characterized by a sharp drop in resistance, started at about 400 °C and 600 °C for  $\text{SrFeO}_{2.5}$  film and  $\text{LaFeO}_3$  film, respectively (shown by the black arrows). It completed at about 550 °C for  $\text{SrFeO}_{2.5}$  film and 650 °C for  $\text{LaFeO}_3$  film, shown by the red arrows. These results suggest the following annealing procedure for the composite films of  $\text{SrFeO}_{2.5}$  /  $\text{LaFeO}_3$  : first anneal the films at temperatures lower than 400 °C for an

appropriate period time to interdiffuse the two compositions, and then anneal them at temperatures higher than 650 °C to ensure the complete crystallization of the composite films. The specific procedure will be determined by further experiments in the next quarter.

## 6. Conclusions

Single phase samples of  $\text{La}_2\text{NiO}_{4+x}$  and  $\text{Pr}_2\text{NiO}_{4+x}$  have been prepared and fully characterized. Dense samples were prepared for conductivity and conductivity relaxation measurements. Conductivity measurements at different  $\text{pO}_2$  values were measured for both samples and reach a maximum of  $\sim 200 \text{ Scm}^{-1}$  sufficient for cathode applications. Conductivity relaxation measurements were made with different pressure switches. The diffusion coefficients are in good agreement with previous measurements by isotope exchange and depth profiling. In contrast the values of  $k_{\text{ex}}$  are much higher for reasons that are not yet well but will be further investigated. Amorphous thin films of  $\text{LaFeO}_3$  and  $\text{SrFeO}_{2.5}$  have been prepared by PLD and their crystallization temperatures determined by measurements of the electrical conductivity as a function of temperature.

## 7. References

1. *Electrochemical Intercalation of Oxygen in  $\text{La}_2\text{NiO}_{4+x}$ : Phase Separation Below Room Temperature*, Yazdi, I.; Bhavaraju, S.; DiCarlo, J. F.; Scarfe, D. P.; Jacobson, A. J., *Chem. Mater.* (1994) 6 2078-2084.
2. *Electrochemical Intercalation of Oxygen in  $\text{Nd}_2\text{NiO}_{4+x}$  ( $0 \leq x \leq 0.18$ ) at 298K*, Bhavaraju, S.; Di Carlo, J. F.; Scarfe, D. P.; Yazdi, I.; Jacobson, A. J., *Chem. Mater.* (1994) 6 2172-2176.
3. *Oxygen diffusion & surface exchange in  $\text{La}_{2-x}\text{Sr}_x\text{NiO}_{4+x}$* , Skinner, S.J.; Kilner, J.A., *Solid State Ionics* (2000) 135 709-712.
4. *Oxygen diffusion and surface exchange in the mixed conducting perovskite  $\text{La}_{0.6}\text{Sr}_{0.4}\text{Fe}_{0.8}\text{Co}_{0.2}\text{O}_{3-x}$* , Benson, S. J.; Chater, R.J.; Kilner, J. A. *Proc. Electrochem. Soc.* (1998) 1997-24 596-609.
5. *Ionic transport in oxygen-hyperstoichiometric phases with  $\text{K}_2\text{NiF}_4$ -type structure*, Kharton, V. V.; Viskup, A. P.; Kovalevsky, A. V.; Naumovich, E. N.; Marques, F. M. B., *Solid State Ionics* (2001) 143 337-353.
6. *Transport and Permeation Properties of  $\text{La}_2\text{NiO}_{4+x}$* , Tichy, R.S.; Huang, K. Q.; Goodenough, J. B.; *Proc. Electrochem. Soc.* (2001) 2000-32 171.
7. *Structure and properties of the Nickel (III) Oxide Family:  $\text{LnSr}_5\text{Ni}_3\text{O}_{11}$* , James, M.; Attfield, J. P.; Rodriguez-Carvajal, J., *Chem. Mater.* (1995) 7 1448.
8. *Synthesis, Structure, and Properties of a Novel Metallic Nickel (III) Oxide,  $\text{CeSr}_7\text{Ni}_4\text{O}_{15}$* , James, M.; Attfield, J. P., *Chem. Mater.* (1995) 7 2338.
9. *Nonstoichiometric  $\text{K}_2\text{NiF}_4$  Type Phases in the Lanthanum Cobalt Oxygen System*, Lewandowski, J. T.; Beyerlein, R. A.; Longo, J. M.; McCauley, R. A., *J. Amer. Ceram. Soc.* (1986) 69 699-703.
10. *An Electrical Conductivity Relaxation Study of  $\text{La}_{0.6}\text{Sr}_{0.4}\text{Fe}_{0.8}\text{Co}_{0.2}\text{O}_{3-x}$* , Wang, S.; van der Heide, P. A. W.; Chavez, C.; Jacobson, A. J.; Adler, S. B. *Solid State Ionics* (2003) 156 201-208.

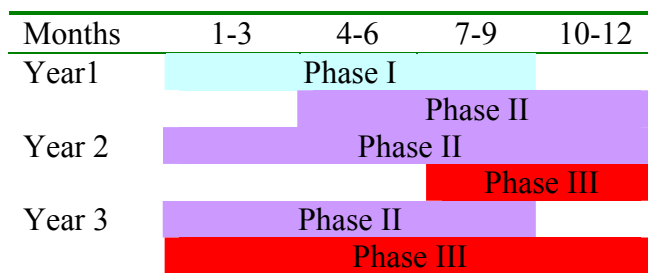
11. *YSZ – Supported Cathodes of Rare Earth Nickelates  $Ln_2NiO_{4+x}$  For ITSOFC (650 °C)*, Bassat, J. M.; Boehm, E.; Grenier, J. C.; Mauvy, F.; Dordor, P.; Pouchard, M., *Fifth European Solid State Fuel Cell Forum*, (2002) 586-593.

## 8 List of Acronyms and Abbreviations

CGO	Cerium Gadolinium Oxide
ECR	Electrical Conductivity Relaxation
EPMA	Electron Probe MicroAnalysis
GDC	Gadolinia Doped Ceria (see CGO)
LSGM	Lanthanum Strontium Magnesium Gallate
PLD	Pulsed Laser Deposition
TGA	Thermogravimetric Analysis
YSZ	Yttria Stabilized Zirconia
IEDP	Isotope Exchange and Depth Profiling

## 9. Milestones and Scope of Work

The project is divided into three phases that will overlap as shown in the timelines below



Phase I: The Phase I objectives are to complete the characterization of a set of perovskite materials for which performance data already exists at PNNL. We will then measure the relevant kinetic parameters. The comparison the real performance data with the fundamental kinetic parameters will be used to guide materials selection in Phase II.

Phase II: The Phase II objectives of the project are to synthesize and characterize new cathode materials and to measure their kinetic parameters. The thermal and chemical compatibility with different electrolytes will be determined. Based on these results, a subset of the best materials will be selected for single cell tests. Some additional compositions will be synthesized if indicated by the single cell test data.

Phase III: The phase three objectives are to evaluate the performance of the best materials identified in Phase I and II. The optimum electrode composition and microstructure will be determined and longer term performance characteristics evaluated.

### Updated Milestones for Year 1

The updated milestones reflect two program adjustments since the original submission. The first is that we have started work on the K1 compositions ahead of the P1 compositions. The latter have been moved into the second half of the first year. The second is that in order to accelerate the thin film materials selection work we have

decided to adopt a combinatorial approach which will permit the simultaneous synthesis of many compositions.

**PHASE I**

Task 1.0 Four modified perovskite oxide compositions (**P1**) selected by UH and PNNL will be synthesized and characterized by X-ray diffraction (XRD) and electron microprobe analysis (EMPA) (Months 6-9)

Task 2.0 The chemical compatibility with YSZ, CGO and LSGM electrolytes will be determined (Months 6-9)

Task 3.0 The temperature dependence of the dc conductivity and stoichiometry will be determined in air for the **P1** compositions. (Months 6-9)

Task 4.0 The diffusion coefficients and surface exchange rates will be measured by electrical conductivity relaxation (Months 6-12)

Task 5.1 Thin films of perovskite compositions will be synthesized by PLD using a combinatorial approach. (Months 3-9) **in progress**

Task 5.2 Electrode-electrolyte interfaces will be characterized for thin films of cathode materials by AC impedance spectroscopy (Months 9-12)

Task 6.0 Electrode-electrolyte interfaces will be characterized for thin films of cathode materials by IEDP (9-12)

**PHASE II**

Task 1.0 Four modified perovskite oxide compositions (**P2**) will be synthesized and characterized by XRD and EMPA (Months 9-12)

Task 1.1 Two  $A_2BO_4$  compositions (**K1**) will be synthesized and characterized by XRD and EMPA. (Months 1-4) **completed**

Task 1.2 Two additional  $A_2BO_4$  compositions (**K2**) will be synthesized and characterized by XRD and EMPA. (Months 6-9)

Task 2.0 The chemical compatibility with YSZ, CGO and LSGM electrolytes will be determined for **P2** (Month 12)

Task 2.1 The chemical compatibility with YSZ, CGO and LSGM electrolytes will be determined for **K1** (Month 7)

Task 2.2 The chemical compatibility with YSZ, CGO and LSGM electrolytes will be determined for **K2** (Month 9)

Task 3.0 The dc conductivity and stoichiometry will be determined in air for the **K1** compositions that have chemical compatibility. (Months 4-6) **completed**

Task 4.0 The diffusion coefficients and surface exchange rates will be measured by electrical conductivity relaxation for the **K1** materials evaluated in Task 3 (Months 6-12). **completed**

Task 4.1  $K_1$  samples will be characterized in symmetric cells by AC impedance spectroscopy (Months 6-9) to confirm the measured values of  $k_{ex}$ .

Task 5.0 Electrode-electrolyte interfaces will be characterized for thin films of cathode materials selected from Task 4.0 by AC impedance spectroscopy (Months 10-33).

Task 6.0 Electrode-electrolyte interfaces will be characterized for thin films of cathode materials selected from Task 4.0 by IEDP (Months 10-33)

Task 7.0 Results from Tasks 4.0, 5.0, and 6.0 will be used as they become available to select cathode electrolyte combinations for single cell tests (Months 10-33).